

# Second-order gravitational effects of local inhomogeneities on CMB anisotropies and non-Gaussian signatures

Kenji Tomita

*Yukawa Institute for Theoretical Physics, Kyoto University, Kyoto 606-8502, Japan*

(Dated: August 7, 2021)

Based on the second-order nonlinear theory of perturbations in non-zero  $\Lambda$  flat cosmological models, we study the gravitational effects of local inhomogeneities on cosmic microwave background (CMB) anisotropies. As the local inhomogeneities we consider firstly large-scale dipole and quadrupole distributions of galaxies around us and next an isolated cluster-scale matter distribution. It is found that, due to the second-order integral Sachs-Wolfe effect, the north-south asymmetry of CMB anisotropies and non-Gaussian signatures (in terms of scale-dependent estimators of kurtosis) in a spot-like object are caused from these matter distributions along light paths. Our theoretical results seem to be consistent with recent various observational results which have been shown by Hansen et al., Eriksen et al., Vielva et al. and Cruz et al.

PACS numbers: 98.80.-k, 98.70.Vc, 04.25.Nx

## I. INTRODUCTION

In the modern precise cosmology, the observations of cosmic microwave background (CMB) anisotropies are bringing us important informations on the structure of the universe [1, 2, 3]. To analyze them, the theories not only of first-order perturbations but also of second-order perturbations are necessary and useful [4]. In a previous paper[5] we studied the general behavior of relativistic second-order perturbations in non-zero  $\Lambda$  flat cosmological models, which correspond to the first-order scalar perturbations, and derived the basic equation for the second-order integral Sachs-Wolfe effect of CMB anisotropies. In the subsequent second previous paper [6] we treated a case when the first-order perturbations consist of primordial random density perturbations and a local inhomogeneity which does not belong to the former perturbations, and derived the second-order temperature perturbations caused by the coupling of the above two types of perturbations. It was found as a result that the nonlinear behavior of the latter temperature perturbations may explain the north-south asymmetry of CMB anisotropies observed by Eriksen et al.[7, 8] and Hansen et al.[9, 10, 11], when we assume a large-scale matter distribution with dipole component around us as a local inhomogeneity.

In this paper, we show in Section II the derivation of power spectra, the possible expansions of anisotropies with spherical harmonics, and the scale-dependent estimator representing non-Gaussian signatures, and consider in Section III a large-scale matter distribution with dipole and quadrupole components around us to bring more realistic north and south asymmetry of CMB anisotropies. To consider non-Gaussian signatures in the spot-like object (which was observed by Vielva et al.[12] and Cruz et al.[13]), moreover, we take up in Section IV a cluster-scale matter distribution which is so isolated to be not included in the primordial random density perturbations, and study its second-order gravitational influence on CMB anisotropies. No non-Gaussian signal is found in the original definition of skewness and kurtosis, but it is shown that a non-Gaussian signal similar to the observed one can be derived in the form of a scale-dependent estimator of kurtosis. Concluding remarks follow in Section V.

## II. CMB ANISOTROPIES WITH SECOND-ORDER NONLINEARITY

### A. Power spectra of CMB anisotropies

The spatially flat background model is assumed and its metric is expressed as

$$ds^2 = g_{\mu\nu} dx^\mu dx^\nu = a^2(\eta)[-d\eta^2 + \delta_{ij} dx^i dx^j], \quad (2.1)$$

where the conformal time  $\eta(= x^0)$  is related to the cosmic time  $t$  by  $dt = a(\eta)d\eta$ , the Greek and Latin letters denote 0, 1, 2, 3 and 1, 2, 3, respectively, and  $\delta_{ij}(= \delta_j^i = \delta^{ij})$  are the Kronecker delta. The matter density  $\rho$  and the scale factor  $a$  have the relations

$$\rho a^2 = 3(a'/a)^2 - \Lambda a^2, \quad \text{and} \quad \rho a^3 = \rho_0, \quad (2.2)$$

where a prime denotes  $\partial/\partial\eta$ ,  $\Lambda$  is the cosmological constant,  $\rho_0$  is an integration constant and the units  $8\pi G = c = 1$  are used.

The first-order and second-order metric perturbations  $\delta_1 g_{\mu\nu}(\equiv h_{\mu\nu})$  and  $\delta_2 g_{\mu\nu}(\equiv \ell_{\mu\nu})$ , respectively, were derived explicitly by imposing the synchronous coordinate condition (in [5]) :

$$h_{00} = h_{0i} = 0 \quad \text{and} \quad \ell_{00} = \ell_{0i} = 0. \quad (2.3)$$

Here only first-order perturbations in the growing mode are shown for the following use. The metric perturbation is

$$h_i^j = P(\eta)F_{,ij}, \quad (2.4)$$

where  $F$  is an arbitrary potential function of spatial coordinates  $x^1, x^2$  and  $x^3$ ,  $h_i^j = \delta^{jl}h_{li}$ , and  $P(\eta)$  satisfies

$$P'' + \frac{2a'}{a}P' - 1 = 0, \quad (2.5)$$

The velocity perturbation  $\delta_1 u^\mu$  vanishes, and the density perturbation is expressed as

$$\delta_1 \rho/\rho = \frac{1}{\rho a^2} \left( \frac{a'}{a} P' - 1 \right) \Delta F. \quad (2.6)$$

Now let us assume a form of the potential function

$$F(\mathbf{x}) = F_P(\mathbf{x}) + F_L(\mathbf{x}) \quad (2.7)$$

with

$$F_P = \int d\mathbf{k} \alpha(\mathbf{k}) e^{i\mathbf{k}\cdot\mathbf{x}} \quad \text{and} \quad F_L = R(r)g(\theta), \quad (2.8)$$

where  $F_P$  is the part of primordial density perturbations with random variables  $\alpha(\mathbf{k})$  and  $F_L$  is the part of local homogeneities with radial and angular dependences specified by  $R(r)$  and  $g(\theta)$ . The latter function is expressed using Legendre polynomials as

$$g(\theta) = \sum_l b_l P_l(\theta) \quad (2.9)$$

and by the averaging process for  $\alpha(\mathbf{k})$ , we have

$$\langle \alpha(\mathbf{k}) \alpha(\mathbf{k}') \rangle = (2\pi)^{-2} \mathcal{P}_F(\mathbf{k}) \delta(\mathbf{k} + \mathbf{k}'). \quad (2.10)$$

The first-order density perturbation corresponding to local inhomogeneities is

$$(\delta_1 \rho/\rho)_L = \frac{1}{\rho a^2} \left( \frac{a'}{a} P' - 1 \right) \tilde{R}(r)g(\theta), \quad (2.11)$$

where

$$\tilde{R}(r) = \frac{1}{r^2} \frac{d}{dr} (r^2 R_{,r}) - \sum_l l(l+1) b_l r^2 R \quad (2.12)$$

with  $R_{,r} \equiv dR/dr$  and  $P' \equiv dP/d\eta$ . The solution for Eq.(2.5) is expressed as

$$\begin{aligned} P &= -\frac{2}{3\Omega_0} y^{-3/2} (\Omega_0 + \lambda_0 y^3) \int_0^y dy' y'^{3/2} / \sqrt{\Omega_0 + \lambda_0 y'^3} + \frac{2}{3\Omega_0} y, \\ \eta &= \int_0^y dy' y'^{-1/2} / \sqrt{\Omega_0 + \lambda_0 y'^3}, \end{aligned} \quad (2.13)$$

where  $y \equiv a/a_0$  is 1 at the present epoch. In sections III and IV, we treat the large-angle case  $g(\theta) = \cos\theta + \beta \cos^2\theta$  and the small-angle case  $g(\theta) = P_l(\theta)$  with  $l = 20$ , respectively.

In the previous paper [6] we derived the temperature perturbations in the first-order and second-order in the case  $g(\theta) = \cos\theta$ . As for the temperature perturbations with general  $g(\theta)$ , we have in the first-order and second-order

$$\begin{aligned}\delta T/T &= \Theta_P + \Theta_L g(\theta), \\ \frac{1}{\delta} T/T &= \Theta_{LP} + \Theta_{LL} + \Theta_{PP},\end{aligned}\quad (2.14)$$

where  $\Theta_P$  and  $\Theta_L$  come from the contributions of only  $F_P$  and  $F_L$ , respectively, and  $\Theta_{PP}$ ,  $\Theta_{LL}$  and  $\Theta_{LP}$  come from the contributions of only  $F_P$ , only  $F_L$  and the coupling of  $F_P$  and  $F_L$ , respectively. In the following,  $\Theta_{PP}$  is neglected because it is small enough, compared with  $\Theta_P$ , and  $\Theta_L$  and  $\Theta_{LL}$  are expressed as

$$\begin{aligned}\Theta_L &= \frac{1}{2} \int_{\lambda_0}^{\lambda_e} d\lambda P'(\eta) R_{,rr}, \\ \Theta_{LL} &= A[g(\theta)]^2 + B[g'(\theta)]^2 + Cg(\theta)[g''(\theta) + \cot\theta g'(\theta)] + D[(g''(\theta))^2 + \cot^2\theta (g'(\theta))^2],\end{aligned}\quad (2.15)$$

where  $\lambda$  is the affine parameter,  $(\eta, r) = (\lambda, \lambda_0 - \lambda)$  along the light path, and  $\lambda_0$  is an observer's value at present. The expressions of  $A, B, C$  and  $D$  are shown in Appendix. Moreover,  $\Theta_P$  and  $\Theta_{LP}$  are

$$\begin{aligned}\Theta_P &= \int d\mathbf{k} \alpha(\mathbf{k}) \sum_l Q_l P_l(\mu), \\ \Theta_{LP} &= \int d\mathbf{k} \alpha(\mathbf{k}) \sum_l \Delta Q_l P_l(\mu) g(\theta),\end{aligned}\quad (2.16)$$

with  $\mu = \mathbf{n} \cdot \mathbf{k}/k$ , where  $\mathbf{n}$  is a directional unit vector with angles  $\theta$  and  $\phi$ . The coefficients are defined as

$$\begin{aligned}Q_l &= \frac{1}{2} (-1)^l (2l+1) \mathcal{H}_P^{(l)}, \\ \Delta Q_l &= \frac{1}{4} (-1)^l (2l+1) \mathcal{H}_{LP}^{(l)},\end{aligned}\quad (2.17)$$

where the expressions of  $\mathcal{H}_P^{(l)}$  and  $\mathcal{H}_{PL}^{(l)}$  are the same as Eqs.(3.6) and (3.12) in the previous paper[6], except for  $\Phi$ . For the above  $g(\theta)$ , we have

$$\begin{aligned}\Phi \equiv & - PP'' R_{,rrr} + \left[ 2P'''P + \frac{1}{2}P' - (P''')_e P \right] R_{,rr} - \frac{1}{2}P'' R_{,r} - P''' R \\ & + P'''' \int_{\lambda_0}^{\lambda} d\bar{\lambda} P R_{,rr} - \frac{1}{7}(3P'P'' + PP''') [4R_{,rr} + 9R_{,r}/r - (6\gamma - 3)R/r^2] \\ & + \frac{2}{7} [(P')^2 + PP''] [4R_{,rrr} + 9R_{,rr}/r - 6(2\gamma - 1)R_{,r}/r^2 + 6(2\gamma - 1)R/r^3] \\ & - \frac{1}{7} PP' [4R_{,rrrr} + 9R_{,rrr}/r - (12\gamma + 3)R_{,rr}/r^2 + 18(2\gamma - 1)R_{,r}/r^3 - 18(2\gamma - 1)R/r^4] \\ & + \frac{3}{7} PP' k^2 [R_{,rr} - R_{,r}/r + (\gamma - 1)R/r^2],\end{aligned}\quad (2.18)$$

where  $\gamma = 2(1 + \beta)$  or  $l(l+1)$  for  $g(\theta) = \cos\theta + \beta \cos^2\theta$  or  $P_l(\theta)$ , respectively.

The power spectra of CMB anisotropies are

$$\begin{aligned}\langle (\delta_1 T/T)^2 \rangle &= \langle (\Theta_P)^2 \rangle + (\Theta_L)^2 g^2(\theta), \\ \langle \delta_1 T/T \delta_2 T/T \rangle &= \langle \Theta_P \Theta_{LP} \rangle + \Theta_L \Theta_{LL} g(\theta)\end{aligned}\quad (2.19)$$

with

$$\begin{aligned}(T_0)^2 \langle (\Theta_P)^2 \rangle &= \sum_l \frac{2l+1}{4\pi} C_l, \\ (T_0)^2 \langle \Theta_P \Theta_{LP} \rangle &= \sum_l \frac{2l+1}{4\pi} \Delta C_l g(\theta),\end{aligned}\quad (2.20)$$

where

$$C_l = (T_0)^2 \int dk k^2 \mathcal{P}_F(k) |\mathcal{H}_P^{(l)}(k)|^2,$$

$$\Delta C_l = \frac{1}{2}(T_0)^2 \int dk k^2 \mathcal{P}_F(k) \mathcal{H}_P^{(l)} \mathcal{H}_{PL}^{(l)}, \quad (2.21)$$

and  $T_0$  is the present CMB temperature. It is important that  $\langle \Theta_P \Theta_{LP} \rangle$  is proportional to  $g(\theta)$  which is the angular component of  $F_L$ .

### B. Expansions of $\Theta_P$ and $\Theta_{LP}$ in terms of spherical harmonics

Let us expand  $\Theta_P$  and  $\Theta_{LP}$  as functions of the directional unit vector  $\mathbf{n}(\theta, \phi)$  as follows:

$$\begin{aligned} \Theta_P(\mathbf{n}) &= \sum_{lm} a_{P,lm} Y_{l,m}(\theta, \phi), \\ \Theta_{LP}(\mathbf{n}) &= \sum_{lm} a_{LP,lm} Y_{l,m}(\theta, \phi), \end{aligned} \quad (2.22)$$

and consider another expansion

$$\Theta_{LP}(\mathbf{n}) = \sum_{lm} b_{LP,lm} g(\theta) Y_{l,m}(\theta, \phi) \quad (2.23)$$

for comparison. Then we have

$$\begin{aligned} a_{P,lm} &= \int Y_{l,m}^*(\theta, \phi) \Theta_P(\mathbf{n}) d\Omega, \\ a_{LP,lm} &= \int Y_{l,m}^*(\theta, \phi) \Theta_{LP}(\mathbf{n}) d\Omega, \\ b_{LP,lm} &= \int Y_{l,m}^*(\theta, \phi) [\Theta_{LP}(\mathbf{n})/g(\theta)] d\Omega, \end{aligned} \quad (2.24)$$

where  $d\Omega = \sin \theta d\theta d\phi$ . Using the relation

$$\int_{-\pi}^{\pi} \int_0^{\pi} Y_{l,m}(\theta, \phi) P_l(\mu) \sin \theta d\theta d\phi = \frac{4\pi}{2l+1} Y_{l,m}(\theta_k, \phi_k), \quad (2.25)$$

we obtain from Eqs.(2.16)

$$\begin{aligned} a_{P,lm} &= \frac{4\pi}{2l+1} \int d\mathbf{k} \alpha(\mathbf{k}) Q_l Y_{l,m}^*(\theta_k, \phi_k), \\ b_{LP,lm} &= \frac{4\pi}{2l+1} \int d\mathbf{k} \alpha(\mathbf{k}) \Delta Q_l Y_{l,m}^*(\theta_k, \phi_k). \end{aligned} \quad (2.26)$$

For  $a_{LP,lm}$ , we consider the case  $g(\theta) = \cos \theta + \beta \cos^2 \theta$  with a constant  $\beta$  for example, and use the relation

$$\cos \theta P_l^m = \frac{1}{2l+1} [(l+m)P_{l-1}^m + (l-m+1)P_{l+1}^m]. \quad (2.27)$$

Then we obtain

$$a_{LP,lm} = a_{LP,lm}^{(1)} + \beta a_{LP,lm}^{(2)}, \quad (2.28)$$

where

$$\begin{aligned} a_{LP,lm}^{(1)} &= \frac{4\pi}{2l+1} N_{l,m} \int d\mathbf{k} \alpha(\mathbf{k}) \left[ \frac{l+m}{2l-1} \frac{\Delta Q_{l-1}}{N_{l-1,m}} Y_{l-1,m}^*(\theta_k, \phi_k) \right. \\ &\quad \left. + \frac{l-m+1}{2l+3} \frac{\Delta Q_{l+1}}{N_{l+1,m}} Y_{l+1,m}^*(\theta_k, \phi_k) \right] \\ a_{LP,lm}^{(2)} &= \frac{4\pi}{2l+1} N_{l,m} \int d\mathbf{k} \alpha(\mathbf{k}) \left\{ \frac{(l+m)(l+m-1)}{2l-1} \frac{\Delta Q_{l-2}}{N_{l-2,m}} Y_{l-2,m}^*(\theta_k, \phi_k) \right. \\ &\quad \left. + \frac{(l-m+1)(l-m+2)}{2l+3} \frac{\Delta Q_{l+2}}{N_{l+2,m}} Y_{l+2,m}^*(\theta_k, \phi_k) \right\} \end{aligned}$$

$$+ \left[ \frac{(l+m)(l-m)}{2l-1} + \frac{(l-m+1)(l+m+1)}{2l+3} \right] \frac{\Delta Q_l}{N_{l,m}} Y_{l,m}^*(\theta_k, \phi_k) \} \quad (2.29)$$

with  $Y_{l,m}(\theta, \phi) = N_{l,m} P_l^m(\theta) e^{im\phi}$  and

$$N_{l,m} \equiv \left[ \frac{2l+1}{2\pi} \frac{(l-m)!}{(l+m)!} \right]^{1/2}. \quad (2.30)$$

When we compare the spatial average of the product  $a_{P,lm}^* \cdot a_{LP,l'm'}$  and that of the product  $a_{P,lm}^* \cdot b_{LP,l'm'}$ , we find a simple expression

$$\langle a_{P,lm}^* b_{LP,l'm'} \rangle \propto \delta_{l,l'} \delta_{m,m'} \quad (2.31)$$

and rather complicated expressions

$$\begin{aligned} \langle a_{P,lm}^* a_{LP,l'm'}^{(1)} \rangle &\propto \text{terms with } \delta_{l,l'\pm 1} \delta_{m,m'}, \\ \langle a_{P,lm}^* a_{LP,l'm'}^{(2)} \rangle &\propto (\text{terms with } \delta_{l,l'} + \text{terms with } \delta_{l,l'\pm 2}) \delta_{m,m'}. \end{aligned} \quad (2.32)$$

Moreover,  $\langle a_{P,lm}^* b_{LP,l'm'} \rangle$  is consistent with  $\Delta C_l$  in Eq.(2.21). The characteristics of north-south asymmetry is, therefore, described more clearly using  $b_{LP,lm}$  than using  $a_{LP,lm}$ , though we can expand the second-order CMB anisotropies in the two forms of expansions ( Eqs.(2.22) and (2.23)).

### C. Non-Gaussian signature

Now let us derive various quantities representing non-Gaussianity. First we consider the dispersion  $\sigma$ . Since  $\langle \delta T/T \rangle = \Theta_{Lg}(\theta) + \Theta_{LL}$ ,  $\sigma$  is defined by

$$\begin{aligned} \sigma^2 &\equiv \langle (\delta T/T - \langle \delta T/T \rangle)^2 \rangle \\ &= \langle (\Theta_P)^2 \rangle^2 + 2\langle \Theta_P \Theta_{LP} \rangle g(\theta). \end{aligned} \quad (2.33)$$

Then we can consider the skewness ( $S$ ) and the kurtosis ( $K$ ) of CMB anisotropies, taking into account the coupling of primordial perturbations ( $P$ ) and local inhomogeneities ( $L$ ) in the second-order. According to the ordinary definitions, they are defined by

$$\begin{aligned} S &\equiv \langle (\delta T/T - \langle \delta T/T \rangle)^3 \rangle / \sigma^3, \\ K &\equiv \langle (\delta T/T - \langle \delta T/T \rangle)^4 \rangle / \sigma^4 - 3. \end{aligned} \quad (2.34)$$

For  $(\delta T/T - \langle \delta T/T \rangle)^2 = (\Theta_P)^2 + 2\Theta_P \Theta_{LP} g(\theta)$ , it is found that both of them vanish.

Here let us consider moreover the expectation values of various scale-dependent estimators  $\bar{\sigma}(\theta)$ ,  $\bar{S}(\theta)$  and  $\bar{K}(\theta)$  in the range of  $\theta$ , which include the estimators due to the spherical Mexican hat wavelet (SMHW). We adopt the northern pole or the center of a cluster-scale as the fixed point. The expectation values are defined in terms of  $\mu \equiv \cos \theta$  as

$$\begin{aligned} [\bar{\sigma}]^2 &= N(\theta_0)^{-1} \int_0^1 d\mu \sigma^2 \psi(\theta, \theta_0) \\ &= \langle (\Theta_P)^2 \rangle + 2\langle \Theta_P \Theta_{LP} \rangle N(\theta_0) \int_0^1 d\mu g(\theta) \psi(\theta, \theta_0), \end{aligned} \quad (2.35)$$

where  $N(\theta_0)$  is the normalization factor given by  $N(\theta_0) = \int_0^1 d\mu \psi(\theta, \theta_0)$ . For SMHW, we have

$$\psi(\theta, \theta_0) \propto (1 + (xR)^2)^2 (2 - x^2)^2 e^{-x^2/2} \quad (2.36)$$

with  $x \equiv (2/R) \tan(\theta/2)$  [14], where  $R$  is the size of Mexican hat related to the angular scale  $\theta_0$ . The expectation values of skewness and kurtosis estimators are expressed as

$$\bar{S}(\theta) = N(\theta_0)^{-1} \int_0^1 d\mu \psi(\theta, \theta_0) \langle (\delta T/T - \langle \delta T/T \rangle)^3 \rangle / [\bar{\sigma}]^3, \quad (2.37)$$

$$\begin{aligned}
\bar{K}(\theta) &= N(\theta_0)^{-1} \int_0^1 d\mu \psi(\theta, \theta_0) \langle (\delta T/T - \langle \delta T/T \rangle)^4 \rangle / [\bar{\sigma}]^4 - 3 \\
&= 3 \left\{ N(\theta_0)^{-1} \int_0^1 d\mu \psi(\theta, \theta_0) [ \langle (\Theta_P)^2 \rangle + 2 \langle \Theta_P \Theta_{LP} \rangle g(\theta) ]^2 - [\bar{\sigma}]^4 \right\} / [\bar{\sigma}]^4.
\end{aligned} \tag{2.38}$$

While  $\bar{S}(\theta)$  vanishes,  $\bar{K}(\theta)$  reduces to

$$\bar{K}(\theta) = 12 \frac{\langle \Theta_P \Theta_{LP} \rangle^2}{[\bar{\sigma}]^4} \left\{ N(\theta_0)^{-1} \int_0^1 d\mu \psi(\theta, \theta_0) [g(\theta)]^2 - \left( N(\theta_0)^{-1} \int_0^1 d\mu \psi(\theta, \theta_0) [g(\theta)] \right)^2 \right\} \tag{2.39}$$

with  $\mu = \cos \theta$ . Here it is to be noticed that, when the third-order terms are taken into account, we have  $\delta_3 T/T = \Theta_{LPP} + \Theta_{LLL} + \Theta_{PLL} + \Theta_{PPP}$  and the terms such as  $\langle (\Theta_P)^2 \rangle \langle \Theta_P \Theta_{PLL} \rangle$  seem to have contributions (to  $\bar{K}$ ) comparable with  $\langle (\Theta_P \Theta_{LP})^2 \rangle$ , but it is found that they are canceled and disappear.

### III. LARGE-SCALE MATTER DISTRIBUTIONS WITH DIPOLE AND QUADRUPOLE SYMMETRIES

In order to study the gravitational effect of a more realistic large-scale structure around us than that in our previous paper, we consider a model with dipole and quadrupole symmetries, in which the angular part of  $F_L(\mathbf{x})$  ( $= R(r)g(\theta)$ ) is

$$g(\theta) = \cos \theta + \beta \cos^2 \theta = \frac{1}{3} [P_0(\mu) + 3P_1(\mu) + 2P_2(\mu)] \tag{3.1}$$

with  $\mu = \cos \theta$  and  $P_l(\mu)$  is the Legendre polynomial. For  $R(r)$  we use the following four types of functions as in the previous paper[6]:

$$\begin{aligned}
R = & R_0 \exp[-\alpha(x-1)^2], \quad \frac{1}{2} R_0 [1 + \cos 2\pi(x-1)], \\
& R_0 x^2 \exp[-\alpha(x-1)^2], \quad \text{and} \quad \frac{1}{2} R_0 x^2 [1 + \cos 2\pi(x-1)]
\end{aligned} \tag{3.2}$$

in the interval  $x = [x_1, x_2]$  with  $x \equiv r/r_c$ , in which  $(x_1, x_2) \equiv (r_1, r_2)/r_c = (0.5, 1.5)$  and  $a_0 r_c$  is  $\approx 300h^{-1} \text{Mpc}$  ( $H_0 = 100h \text{ km/s/Mpc}$ ). In all types we have  $R = 0$  for  $x > x_2$  or  $x < x_1$ .  $R_0$  is the normalization constant and a constant  $\alpha$  is chosen as 20.

The above functions were chosen so that they have radially convex behaviors and the first two of them are symmetric for  $x > 1$  and  $x < 1$ , while the last two have small asymmetry.

The powers of CMB anisotropies are calculated using Eqs.(2.20) and (2.21) for  $l = 1 - 22$ . The values of  $l(l+1)C_l \xi$  and  $l(l+1)\Delta C_l \xi / R_0$  for  $\beta = -0.3$  are shown in Table I, in which G, S, MG and MS represent the Gaussian type (G), the sine type (S), the modified Gaussian type (MG) and the modified sine type (MS). Here  $\xi \equiv 2\pi / [\mathcal{P}_{F0}(T_0)^2]$  and  $\mathcal{P}_{F0} = 2.1 \times 10^{-8}$ .

In Fig. 1, the behaviors of  $l(l+1)[C_l + 2\Delta C_l g(\theta)](\mu K)^2$  in the northern and southern poles are shown for  $\beta = -0.3$ , in which we used the mean of four types. We plotted  $l(l+1)[C_l + 2\overline{\Delta C_l} g(\theta)]$  for  $l = 3, 6, 9, \dots, 21$ , where  $\overline{\Delta C_l} \equiv (\Delta C_{l-1} + \Delta C_l + \Delta C_{l+1})/3$ . For  $R_0$ , we adopted in the following  $R_0 = -2.3 \times 10^{-5}$ , which was obtained as the best value in the previous paper. For  $\beta >$  and  $< 0$ , the deviation of  $l(l+1)[C_l + 2\Delta C_l g(\theta)]$  in the northern pole from  $l(l+1)C_l$  is larger and smaller than that in the southern pole, respectively. It is found from this figure that our model is at least qualitatively consistent with Fig.2 in Eriksen et al.'s paper[7]. In Table II,  $\Theta_L/R_0, A/(R_0)^2, B/(R_0)^2, C/(R_0)^2$  and  $D/(R_0)^2$  are shown for  $\beta = -0.3$ .

Next let us evaluate the scale-dependent estimators of skewness and kurtosis. Since  $\bar{S}(\theta)$  vanishes, we consider only  $\bar{K}(\theta)$ . As the essential property does not seem to depend on the details of function  $\psi(\theta, \theta_0)$ , we assume here that it is expressed as

$$\psi(\theta, \theta_0) = 1 \text{ for } 0 \leq \theta \leq \theta_0, \text{ and } \psi(\theta, \theta_0) = 0 \text{ for } \theta > \theta_0, \tag{3.3}$$

and that  $N(\theta_0) = 1 - \cos \theta_0$ . Then we obtain for  $g(\theta) = \cos \theta + \beta \cos^2 \theta$  from Eq.(2.39):

$$\bar{K}(\theta) = \zeta^2 \left( \frac{\langle \Theta_P \Theta_{PL} \rangle}{\langle \Theta_P \rangle^2} \right)^2 (1 - \mu)^2 \left[ 1 + 2\beta(1 + \mu) + \frac{4}{15} \beta^2 (4 + 7\mu + 4\mu^2) \right] / \left\{ 1 + \zeta \left[ 1 + \mu + \frac{2}{3} \beta (1 + \mu + \mu^2) \right] \right\}^2, \tag{3.4}$$

TABLE I: CMB anisotropy powers  $l(l+1)C_l$  and  $l(l+1)\Delta C_l$  in the case  $\beta = -0.3$  and  $n = 0.97$ . The latter is caused by the coupling of cosmological perturbations and local inhomogeneities of types G, S, MG and MS. Here  $\xi \equiv 2\pi/[\mathcal{P}_{F0}(T_0)^2]$ , and  $\mathcal{P}_{F0}$  and  $R_0$  are the normalization factors.

$l$	$l(l+1)C_l\xi$	$10^{-3} \times 2l(l+1)\Delta C_l\xi/R_0$				mean
		G	S	MG	MS	
1	4.550	-0.78	-1.98	-0.76	-1.43	-1.24
2	0.184	-0.49	-0.53	-0.44	-0.49	-0.49
3	0.177	0.57	-0.026	0.75	0.10	0.35
4	0.170	-0.59	-0.77	-0.039	-0.13	-0.38
5	0.168	2.00	0.18	1.69	0.22	1.02
6	0.166	1.88	0.82	2.58	1.86	1.79
7	0.167	2.41	1.20	0.094	-0.17	0.88
8	0.165	3.09	1.37	2.29	0.60	1.84
9	0.172	-5.14	-3.37	-7.39	-3.73	-4.91
10	0.173	-1.26	-0.76	-3.24	-3.10	-2.09
11	0.179	-5.01	1.07	-1.63	3.50	-0.52
12	0.176	-4.25	-1.72	-3.26	0.51	-2.18
13	0.191	5.76	3.63	10.61	3.20	5.80
14	0.191	4.60	3.16	6.47	7.82	5.51
15	0.203	7.21	-9.53	4.47	-9.62	-1.87
16	0.197	2.39	3.36	0.39	-0.86	1.32
17	0.215	-1.56	10.28	-11.15	3.57	0.28
18	0.220	-4.54	-1.61	-4.00	-3.87	-3.50
19	0.230	-19.91	-8.12	-8.58	1.13	-8.87
20	0.231	2.77	-6.63	3.63	2.08	0.46
21	0.240	33.138	13.66	35.62	13.42	23.96
22	0.260	2.94	13.74	-0.38	1.95	4.56

TABLE II: CMB anisotropies caused by only the spot-like object of types G, S, MG and MS.  $R_0$  is the normalization factor.

model types	G	S	MG	MS	mean
$\Theta_L/R_0$	0.75	0.022	0.92	0.23	0.48
$A/(R_0)^2$	$2.5 \times 10^4$	$1.5 \times 10^4$	$3.0 \times 10^4$	$2.3 \times 10^4$	$2.3 \times 10^4$
$B/(R_0)^2$	$-9.1 \times 10^2$	$-9.1 \times 10^2$	$-9.1 \times 10^2$	$-8.7 \times 10^2$	$-9.0 \times 10^2$
$C/(R_0)^2$	31	45	27	36	35
$D/(R_0)^2$	10	15	8.9	11	11

where

$$\zeta \equiv \frac{\langle \Theta_P \Theta_{PL} \rangle}{\langle (\Theta_P)^2 \rangle} \quad (3.5)$$

with  $\mu = \cos\theta$ .  $\langle (\Theta_P)^2 \rangle$  and  $\langle \Theta_{PL} \rangle$  are derived from Eq.(2.20). In the case  $\beta = 0$ ,  $\zeta$  is  $-0.0624, -0.0143, -0.0666, -0.0222$  for G, S, MG, MS, respectively. In the case  $\beta = -0.3$ ,  $\zeta$  is  $-0.0787, -0.0352, -0.0813, -0.407$  for G, S, MG, MS, respectively. The scale-dependent estimator of kurtosis vanishes at  $\theta = 0$  (the north pole) and increases with the increase of  $\theta$ . But it is of the order of at most  $4.0 \times 10^{-3} \ll 1$ .

#### IV. A CLUSTER-SCALE SPOT-LIKE OBJECT

In this section we study the anisotropy of CMB radiation, coming through the inside or neighborhood of an isolated cluster-scale object, to consider non-Gaussian signatures of the spot-like object [12, 13]. The distance to the object is about  $30h^{-1}\text{Mpc}$  and the angular radius is about 7 degree.

The angular part of  $F_L(\mathbf{x})(= R(r)g(\theta))$  is assumed to be

$$g(\theta) = P_{l_1}(\cos \theta), \text{ for } 0 \leq \theta \leq \theta_1, \text{ and } g(\theta) = 0 \text{ for } \theta > \theta_1, \quad (4.1)$$

respectively, with  $l_1 = 20$ , where  $\cos \theta_1 = 0.992$  or  $\theta_1 = 7.25\text{deg}$ . The radial part  $R(r)$  is assumed to have the four types G, S, MG and MS (cf. Eq.(3.2), in which  $(x_1, x_2) = (r_1, r_2)/r_c = (0.9, 1.1)$  and  $(ar_c) \approx 30h^{-1}\text{Mpc}$ .

The powers of CMB anisotropies are calculated using Eqs. (2.20) and (2.21) for  $l = 1 \sim 40$ , similarly to those in Section III. In Table III, the values of  $l(l+1)\Delta C_l$  are shown for  $l = 1 - 22$ . It seems that there is an oscillatory behavior with the period of  $\Delta l \simeq 5$ . In Table IV,  $\Theta_L/R_0, A/(R_0)^2, B/(R_0)^2, C/(R_0)^2$  and  $D/(R_0)^2$  are shown.

Now let us derive the scale-dependent estimator of kurtosis

$$\bar{K}(\theta) = \zeta^2 \Phi(\theta) / [1 + 2\zeta \Psi(\theta)]^2, \quad (4.2)$$

where  $\zeta$  is defined by Eq.(3.5) and

$$\begin{aligned} \Phi(\theta) &\equiv 12 \left\{ N(\theta, \theta_0)^{-1} \int_0^1 [g(\theta')]^2 \psi(\theta', \theta_0) d\mu' - \Psi^2 \right\}, \\ \Psi(\theta) &\equiv N(\theta, \theta_0)^{-1} \int_0^1 g(\theta') \psi(\theta', \theta_0) d\mu' \end{aligned} \quad (4.3)$$

with  $\mu' = \cos \theta'$ . The value of  $\zeta/R_0$  is  $-(4.8, 2.9, 2.4, 3.0) \times 10^6$  for G, S, MG and MS, respectively, and their mean is  $-3.2 \times 10^6$ . As the fix point we adopt here the center of the cluster-scale object.

To determine  $R_0$ , we consider here the first-order density perturbation due to the cluster-scale object. It is expressed as

$$(\delta_1 \rho / \rho)_L = \frac{1}{\rho a^2} \left( \frac{a'}{a} P' - 1 \right) \tilde{R} P_{l_1}(\cos \theta) \quad (4.4)$$

with  $l_1 = 20$ , where

$$\tilde{R} = (r_c)^{-2} [(x^2 R_{,x})_{,x} / x^2 - l_1(l_1 + 1)R/x^2]. \quad (4.5)$$

The ratio  $(\delta M/M)$  of perturbed mass ( $\delta M$ ) to background mass ( $M$ ) in the interval  $x = [x_1, x_2]$  is defined by

$$\begin{aligned} J &\equiv \int_{x_1}^{x_2} \int_0^1 (\delta_1 \rho / \rho)_L x^2 dx d\mu / \left\{ \frac{1}{3} [(x_2)^3 - (x_1)^3] \int_0^1 d\mu \right\} \\ &= \frac{3}{2(\rho a^2)_0 (r_c)^2} \left( \frac{a'}{a} P' - 1 \right)_0 [(x_2)^3 - (x_1)^3]^{-1} \int_{x_1}^{x_2} [(x^2 R_{,x})_{,x} - l_1(l_1 + 1)R] dx. \end{aligned} \quad (4.6)$$

The factor  $[(a'/a)P' - 1]_0$  is equal to  $-0.456$  in the concordant background model with  $\Omega_0 = 0.27$  and  $\Lambda_0 = 0.73$ , and we have

$$J = -3.9 \times 10^3 (30h^{-1}\text{Mpc}/a_0 r_c)^2 \int_{x_1}^{x_2} [(x^2 R_{,x})_{,x} - l_1(l_1 + 1)R] dx. \quad (4.7)$$

After performing the integration in Eq.(4.7), we obtain

$$J = (2.5, 0.94, 3.1, 1.9) \times 10^4 R_0 (30h^{-1}\text{Mpc}/a_0 r_c)^2, \quad (4.8)$$

for types G, S, MG and MS, respectively, and their mean value is  $\bar{J} = 2.1 \times 10^4 R_0 (30h^{-1}\text{Mpc}/a_0 r_c)^2$ .

On the other hand, the observed value of  $\langle (\delta M/M)^2 \rangle^{1/2}$  is about 1 on the scale of  $8h^{-1}\text{Mpc}$  and for the power spectrum  $P(k) \propto k^n$ , we have  $\delta M/M \propto M^{-(n+3)/6} \propto r^{-(n+3)/2} = r^{-1.985}$  for  $n = 0.97$ . Since we are considering a local inhomogeneity included in the sphere of radius  $2a_0 r_c$ , its scale is regarded as  $4\epsilon a_0 r_c$  ( $\simeq 120\epsilon h^{-1}\text{Mpc}$ ) with  $\epsilon \approx 1$ , so that the value of  $\delta M/M$  for the inhomogeneity is

$$(\delta M/M)_{\text{power}} = (8h^{-1}/4\epsilon a_0 r_c)^{1.985} / b = 4.6 \times 10^{-3} (b\epsilon^{1.985})^{-1} (30h^{-1}\text{Mpc}/a_0 r_c)^{1.985}, \quad (4.9)$$

where  $b$  is the biasing factor[15, 16]. If we assume  $|\bar{J}| = (\delta M/M)_{\text{power}}$ , we obtain from Eq.(4.9)

$$R_0 = 2.2 \times 10^{-7} (b\epsilon^{1.985})^{-1} (30h^{-1}\text{Mpc}/a_0 r_c)^{0.015}. \quad (4.10)$$



TABLE III: CMB anisotropy powers  $l(l+1)C_l$  and  $l(l+1)\Delta C_l$  in the cluster-scale case  $n = 0.97$ . The latter is caused by the coupling of cosmological perturbations and the cluster-scale inhomogeneity of types G, S, MG and MS. Here  $\xi \equiv 2\pi/[\mathcal{P}_{F0}(T_0)^2]$ , and  $\mathcal{P}_{F0}$  and  $R_0$  are the normalization factors.

$l$	$l(l+1)C_l\xi$	$10^{-5} \times 2l(l+1)\Delta C_l\xi/R_0$				mean
		G	S	MG	MS	
1	4.550	-304.8	-173.8	-135.1	-171.3	-196.3
2	0.184	-7.96	-4.71	-3.81	-4.84	-5.33
3	0.177	-10.44	-6.32	-5.15	-6.51	-7.11
4	0.170	-11.94	-7.43	-6.17	-7.77	-8.33
5	0.168	-19.05	-11.40	-9.04	-11.34	-12.71
6	0.166	-17.96	-11.24	-9.11	-11.33	-12.41
7	0.167	-1.60	-1.06	-0.70	-0.73	-1.02
8	0.165	-6.36	-4.27	-3.30	-3.90	-4.46
9	0.172	-4.19	-3.14	-2.84	-3.50	-3.42
10	0.173	-1.62	-1.41	-1.32	-1.54	-1.47
11	0.179	-17.75	-10.95	-8.80	-10.93	-12.11
12	0.176	-16.40	-9.29	-7.29	-9.22	-10.55
13	0.191	5.74	2.75	2.01	2.70	3.30
14	0.191	13.41	7.34	5.20	6.58	8.13
15	0.203	-8.28	-6.40	-5.98	-7.38	-7.01
16	0.197	-22.76	-14.10	-11.73	-14.67	-15.82
17	0.215	-17.28	-8.55	-5.74	-7.30	-9.72
18	0.220	13.28	9.04	7.68	9.71	9.93
19	0.230	27.03	16.66	12.82	15.77	17.32
20	0.231	-12.86	-5.15	-3.62	-5.02	-6.67
21	0.240	-35.12	-22.95	-19.08	23.70	-13.36
22	0.260	-0.663	-1.99	0.350	0.614	-0.42

TABLE IV: CMB anisotropies caused by only the spot-like object of types G, S, MG and MS.  $R_0$  is the normalization factor.

model types	G	S	MG	MS	mean
$\Theta_L/R_0$	179.	-0.104	1.66	0.313	45.3
$A/(R_0)^2$	$-9.1 \times 10^8$	$-4.2 \times 10^8$	$-3.1 \times 10^8$	$-4.4 \times 10^8$	$-4.2 \times 10^8$
$B/(R_0)^2$	$-1.4 \times 10^5$	$-1.5 \times 10^5$	$-1.8 \times 10^5$	$-1.7 \times 10^5$	$-1.6 \times 10^5$
$C/(R_0)^2$	$3.1 \times 10^{-3}$	$3.5 \times 10^{-4}$	$2.8 \times 10^{-4}$	$3.9 \times 10^{-4}$	$1.0 \times 10^{-3}$
$D/(R_0)^2$	$6.3 \times 10^3$	$2.6 \times 10^3$	$2.0 \times 10^3$	$2.7 \times 10^3$	$3.4 \times 10^3$

Accordingly it is reasonable to treat the case with  $R_0 = (2 \sim 3) \times 10^{-7}$ .

Now let us show the behavior of the scale-dependent estimator of skewness and kurtosis. Since the skewness estimator vanishes, we consider only  $\bar{K}(\theta)$  for  $R_0 = (2.5, 2.6, 2.7) \times 10^{-7}$ . Here we assume the simple functional form Eq.(3.3) for  $\psi(\theta, \theta_0)$  and  $N(\theta_0) = 1 - \cos \theta_0$  in a similar way to the previous section. Then the behavior of  $\bar{K}$  is shown in Fig. 2 and the peak of the kurtosis is found to appear around  $\theta \approx 3.5$  deg, and so the diameter ( $2\theta$ ) of the circular region with the peak is about 7 deg. The estimator of dispersion  $\bar{\sigma}(\theta)$  (being the denominator of Eq.(4.2)) decreases and so  $\bar{K}(\theta)$  increases with the increase of  $R_0$  around these values. The values of the kurtosis at the peaks are 1.3, 0.81, 0.55 for  $R_0 = (2.5, 2.6, 2.7) \times 10^{-7}$ , respectively. It is therefore found from this figure that the case  $R_0 = 2.6 \times 10^{-7}$  is best to represent the observed kurtosis [12, 13].

Thus we found that the scale-dependent estimator of kurtosis does not vanish, though kurtosis in the original definition vanishes. The origin of this strange situation may be in the definition of the estimator (Eq.(2.38)) and Vielva et al's definition (Eq.(18) in [12]) which are given as the ratio of the two expectation values.

## V. CONCLUDING REMARKS

The large-scale local inhomogeneity with the north-south asymmetry was found to reproduce the observed asymmetry of CMB anisotropies in the  $l(l+1)(C_l + 2\Delta C_l g(\theta))$  diagram in the case when not only a dipole component but also a small quadrupole component are included. It is interesting that through the second-order nonlinearity, the asymmetry in the CMB anisotropies observed in WMAP may be related to the asymmetry in a large-scale structure observed in SDSS.

In our models of large-scale and cluster-scale inhomogeneities, the skewness and kurtosis in the original definition vanish, but a non-Gaussian signal similar to that observed in the spot-like object[12] was found to be theoretically derived in our model by using the scale-dependent estimator of kurtosis. It may, therefore, be difficult to conclude the existence of pure non-Gaussianity from obtaining observationally the non-vanishing values of scale-dependent estimators of skewness and kurtosis.

In the large-scale and cluster-scale cases, the dependence of our results on  $ar_c$  is very small, and that on  $x_1$  and  $x_2$  also is qualitatively small, though quantitatively sensitive.

It is emphasized finally that the local inhomogeneities we considered in our models are not any extraordinary outliers, but usual inhomogeneities with ordinary mass spectra, and that their important unique character may be so near and isolated that they can be regarded as being not included in the primordial random perturbations. In the cluster-like object, it is additionally required that the dispersion ( $\bar{\sigma}$ ) is comparatively small, to show a remarkable spot-like appearance.

### Acknowledgments

The author thanks E. Komatsu for helpful discussions on the harmonic expansion of second-order anisotropies. He also thanks K.T. Inoue for various discussions on the observed asymmetry of CMB anisotropies. Numerical computation in this work was carried out at the Yukawa Institute Computer Facility.

### APPENDIX A: DERIVATION OF $\Theta_{LL}$

$$\Theta_{LL} = Ag^2 + B(g')^2 + Cg(g'' + \cot \theta g') + D[(g'')^2 + \cot^2 \theta (g')^2], \quad (\text{A1})$$

where

$$\begin{aligned} A &= \frac{1}{8} \left( \int_{\lambda_o}^{\lambda_e} d\lambda P' R_{,rr} \right)^2 - \frac{1}{4} \int_{\lambda_o}^{\lambda_e} d\lambda PP'(R_{,rr})^2 \\ &+ \frac{1}{4} \int_{\lambda_o}^{\lambda_e} d\lambda P'' R_{,rr} \int_{\lambda_o}^{\lambda} d\bar{\lambda} P(\bar{\eta}) R_{,rr}(\bar{r}) \\ &+ \frac{1}{4} \int_{\lambda_o}^{\lambda_e} d\lambda \left\{ -P' \left[ RR_{,rr} + \frac{5}{4} (R_{,r})^2 \right] \right. \\ &+ \left. \frac{1}{14} PP' [19(R_{,rr})^2 - 12\tilde{R}R_{,rr} - 3(R_{,rr} + \tilde{R})(R_{,rr} - \tilde{R}) - 6(R_{,r}/r)^2] \right\}, \\ B &= \frac{1}{4} \int_{\lambda_o}^{\lambda_e} d\lambda \left\{ \frac{1}{4} P' R^2 / r^4 + \frac{1}{14} PP' [19(R_{,r}/r)^2 - 6(R_{,r}/r - R/r^2)] \right\}, \\ C &= -\frac{3}{28} \int_{\lambda_o}^{\lambda_e} d\lambda PP' RR_{,r} / r^3, \\ D &= -\frac{3}{56} \int_{\lambda_o}^{\lambda_e} d\lambda PP'(R/r^2)^2. \end{aligned} \quad (\text{A2})$$

- 
- [1] C.L. Bennet et al., *Astrophys. J. Suppl.* **148**, 1 (2003).
  - [2] D.N. Spergel et al., *Astrophys. J. Suppl.* **148**, 175 (2003).
  - [3] E. Komatsu et al., *Astrophys. J. Suppl.* **148**, 119 (2003).

- [4] N. Bartolo, E. Komatsu, S. Matarrese and A. Riotto, *Phys. Rep.* **402**, 103 (2004).
- [5] K. Tomita, *Phys. Rev.* **D71**, 083504 (2005).
- [6] K. Tomita, *Phys. Rev.* **D72**, 043526 (2005).
- [7] H.K. Eriksen, D.I. Novikov, P.B. Lilje, A.J. Banday and K.M. Górski, *Astrophys. J.* **605**, 14 (2004).
- [8] H.K. Eriksen, D.I. Novikov, P.B. Lilje, A.J. Banday and K.M. Górski, *Astrophys. J.* **612**, 64 (2004).
- [9] F.K. Hansen, A.J. Banday and K.M. Górski, *Mon. Not. R. Astron. Soc.* **354**, 641 (2004).
- [10] F.K. Hansen, A. Balbi, A.J. Banday and K.M. Górski, *Mon. Not. R. Astron. Soc.* **354**, 905 (2004).
- [11] F.K. Hansen, P. Cabella, D. Marinucci and N. Vittorio, *Astrophys. J.* **607**, L67 (2004).
- [12] P. Vielva et al., *Astrophys. J.* **609**, 22 (2004).
- [13] M. Cruz et al., *Mon. Not. R. Astron. Soc.* **356**, 29 (2005).
- [14] E. Martínez-González et al., *Mon. Not. R. Astron. Soc.* **336**, 22 (2002).
- [15] Y. Suto, *Prog. Theor. Phys.* **90**, 1173 (1993).
- [16] A.R. Liddle and D.H. Lyth, *Cosmological Inflation and Large-Scale Structure* (Cambridge Univ. Press, Cambridge, United Kingdom, 2000), p 264.

FIG. 1: The  $l$  dependence of  $l(l+1)[C_l + 2\delta C_l g(\theta)]$  in the northern pole ( $\theta = 0$ ) and southern pole ( $\theta = \pi$ ).

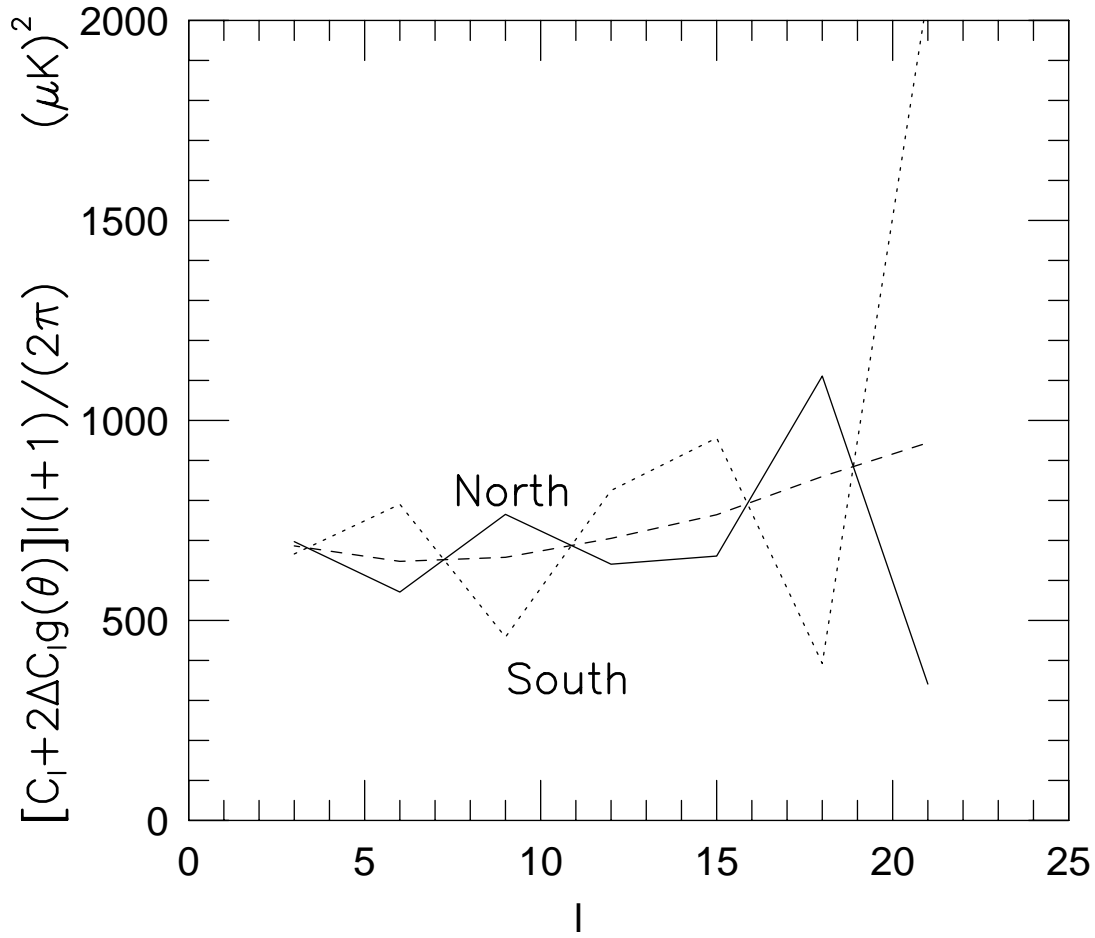


FIG. 2: The angular dependence of the scale-dependent estimator of kurtosis.

